VERSITA
Construction Science
10.2478/cons-2013-0008
2013 /14

# Microstructural Investigations of Ultra-High Performance Concrete Obtained by Pressure Application within the First 24 Hours of Hardening

Janis Justs[1], Diana Bajare[2], Aleksandrs Korjakins[3], Gundars Mezinskis[4], Janis Locs[5], Girts Bumanis[6], [1-6] *Riga Technical University*

***Abstract.*** **In this study, the effect of pressure application (0–50 MPa) to fresh concrete right after casting and during the first 24 hours of hardening has been examined. Supplementary cementitious materials in a form of silica fume, nanosilica and ground quartz sand were used. The aim of pressure application was to reduce porosity, thus improving concrete mechanical properties. Considerable reduction in porosity and a subsequent increase in compressive strength reaching the level of Ultra-High Performance Concrete (UHPC) were achieved. Mechanical and physical properties were tested and gas sorption porosimetry, mercury intrusion porosimetry (MIP), X-ray diffraction (XRD), as well as scanning electron microscopy (SEM) were used for material characterization.**

***Keywords:*** **Ultra-High Performance Concrete (UHPC), pressure application, porosity, compressive strength**

## I. Introduction

Ultra-high performance concrete (UHPC) is a modern building material with superior properties. such as high compressive strength, high modulus of elasticity, low permeability and excellent durability. All these properties can be achieved taking into account some basic principles and processing methods that can be listed as follows: (i) minimizing defect occurrence in a concrete matrix and obtaining maximum density by optimizing particle size distribution; (ii) minimizing water/cement ratio by the use of water reducing admixtures; (iii) using pozzolanic materials, such as silica fume, to fill voids between larger particles, to improve rheological properties and to enhance secondary calcium silicate hydrate formation; (iv) incorporation of steel fibers to prevent brittle failure and polypropylene fibers, to increase UHPC fire resistance [1-6].

In 1994 Richard and Cheyrezy [5] produced reactive powder concrete (RPC) with the compressive strength of 800 MPa. RPC is a type of UHPC that is characterized by very fine particles, and no coarse aggregate is present. Production technology included pressure application and heat treatment.

First demonstrations of UHPC outside laboratory were in footbridges. These structures appeared at the end of 1990s. Some of the most well-known examples are in Sherbrook (1997), Seoul (2002) and Kassel (2007) [7-9]. The first two road bridges using UHPC with the compressive strength of more than 170 MPa were built in France in 2001 (Bourg-lès-Valence bypass) [10].

There are examples of commercially available UHPC that is used in the construction industry today. One such example is Ductal®. The Ductal® technology was developed by the combined efforts of three companies: Lafarge – the construction materials manufacturer, Bouygues – the contractor in civil and structural engineering and Rhodia – the chemical materials manufacturer [11].

The aim of this study is to investigate the influence of pressure applied during the sample hardening process. Concrete mix composition with the designed compressive strength of approximately 100 MPa at 28 days was selected as a basic mix. Pressure has been applied right after casting in order to improve concrete properties. Mechanical strength of prepared samples was compared. By pressing concrete in the fresh state, most of entrapped air can be eliminated and pore diameters reduced. Distance between particles determines most of the concrete properties. Elimination of voids and reduction of pore diameters would result in enhancement of concrete performance [12; 13]. As the macroscopic properties of UHPC are related to its microstructure, porosity, pore-size distributions as well as morphology of hydration products were analysed by using SEM and Hg porosimetry. UHPC strength border of 150 MPa was reached by applying the pressure of 50 MPa.

## II. Materials and Methods

### *A. Materials*

The materials used in this study were commercially available raw materials, cementitious materials and admixtures. Chemical composition of CEM I 42.5 N Portland cement was tested according to the standard LVS EN 196-2:2005, and results are given in Table 1.

The initial cement setting time was 182 min and the final setting – 224 min (according to LVS EN 196-3:2005), the normal consistency was 28.2% (according to LVS EN 196-3:2005).

Blaine fineness of cement was 3787cm$^2$/g (according to LVS EN 196-6:2010). Na equivalent was 1.68. Compressive strength after 1 day was 15.4 MPa, after 2 days – 32.9 MPa, after 7 days – 48.8 MPa and after 28 days – 60.5 MPa.

TABLE I
CHEMICAL COMPOSITION OF CEMENT AND POZZOLANIC ADDITIVES, [WEIGHT %]

| | Silica fume* | Nanosilica** | Cement |
|---|---|---|---|
| $SiO_2$ | 98.4 | 99.99 | 18.85 |
| $Al_2O_3$ | 0.20 | | 4.37 |
| $Fe_2O_3$ | 0.01 | | 3.09 |
| CaO | 0.20 | | 61.98 |
| MgO | 0.10 | | 3.64 |
| $SO_3$ | 0.10 | | 3.18 |
| $Na_2O$ | 0.15 | | 0.22 |
| $K_2O$ | 0.20 | | 1.25 |
| $TiO_2$ | | | 0.32 |
| Cl | | | 0.08 |
| $P_2O_5$ | | | 0.06 |
| $Mn_2O_3$ | | | 0.08 |
| Other | 0.60 | | 2.88 |
| Total | 100.00 | 100 | 100.00 |

*From Elkem Microsilica 971material datasheet
** From Elkem NanoSilica 999 material datasheet

According to material datasheet, 100% of nanosilica particles had sizes below 400 nm and 99.8% of silica fume particles were smaller than 45 µm. 90% of silica fume particles had dimensions ranging from 20 nm to 0.5 µm, but size of nanosilica particles was in the interval between 20 and 100 nm. Polycarboxylate ether based superplasticizer (PCE) was used. The W/C ratio was 0.25. Basic concrete mix was designed in order to provide 28-day compressive strength in the range of 100 MPa. Mix composition is given in Table 2.

TABLE II
CONCRETE MIX COMPOSITION

| Material | Quantity, kg/m$^3$ |
|---|---|
| Cement CEM I 42,5 N | 800 |
| Sand 0.3-2.5 mm | 510 |
| Sand 0-1.0 mm | 480 |
| Ground quartz sand | 200 |
| Silica fume | 100 |
| Nanosilica | 20 |
| Superplasticizer | 20 |
| Water | 200 |

### *B. Particle Size Distribution*

Grading of materials is essential to produce UHPC. Particle size distribution of sand was obtained by sieving. Ground quartz sand particle size distribution was measured by particle size and Zeta potential analyzers "90 Plus MAS, ZetaPALS Brookhaven Industries".

To optimize packing of available materials down to nano-scale, software from Elkem materials based on modified Andreassen particle packing model [3] was used (curve parameters q=0.25, $D_{max}$ = 2.5 mm and $D_{min}$ = 0.0001 mm were selected).

Particle size distribution curve of the selected mix is given in Fig. 1.

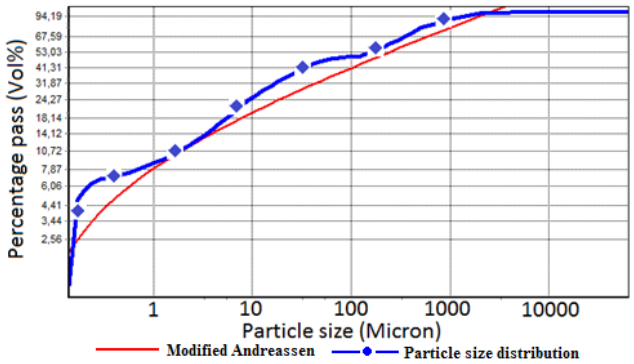


Fig. 1. Particle size distribution of the selected concrete mix.

### *C. Mixing Procedure*

The mixing procedure of materials was the following: all dry materials were mixed by a high speed electric paddle mixer until a homogenous mixture was obtained (for 1 min). Then water and superplasticizer were added in two steps. During the first step 70% of water was added and the batch was mixed for 1.5 minutes. During the second step the rest of the water together with the full amount of superplasticizer was added. Mix with the cone slump of class S2 (according to LVS EN 12350-2) was obtained at the end of mixing. Total mixing time was approximately 6 minutes.

### *D. Experimental Setup*

The experimental setup for pressure applied cylindrical specimen with a diameter of 50 mm and height of 100 mm is shown in Fig. 2.

Fig. 2. Experimental setup for pressure application to the specimens.

Customized cylindrical mold with an inner diameter of 50 mm and adjustable height was designed and produced for the current study. The mold consisted of 3 high precision details: a central cylinder and two pistons closing the cylinder from both ends. In order to remove the entrapped air and reduce pore sizes, pressure of 10, 20, 30, 40 and 50 MPa was applied by a manual hydraulic press right after concrete casting and retained constant for 24 hours. Due to relatively low W/C ratio (0.25), little to no excess water was observed. Pressure

readings were taken from the manometer installed on top of the press.

After the first 24 hours pressure was removed and the specimens were remolded and cured in the water at the temperature of 20˚C until the age of 28 days.

### *E. Testing Methods of Concrete*

Mechanical, physical and microstructural investigations were carried out for specimens at the age of 28 days and 6 months.

Mechanical properties were determined according to LVS EN 12390-3:2009 "Testing hardened concrete – Part 3: Compressive strength of test specimens".

Density was detremined according to LVS EN 12390-7:2009 "Testing hardened concrete – Part 7: Density of hardened concrete". Porosity was detremined according to ASTM C642-06 Standard Test Method for Density, Absorption, and Voids in Hardened Concrete.

Pore volume and pore sizes were determined by Porosimeter NOVA 1200E (0.35–200 nm) "Quantachrome Instruments" and Hg Porosimeter Pore Master 33 (0.0064–950 μm) "Quantachrome Instruments". The samples were observed by the field emission scanning electron microscope Mira\LMU "Tescan", and the elemental composition of the observed phases was assessed by the energy dispersive X-ray spectrometrer (EDX) Inca 350 "Oxford instruments" installed on the scanning electron microscope. Mineralogical composition of UHPC specimens was determined by X-Ray diffractometer "RIGAKUULTIMA+".

## III. Results and Discussion

### *A. Macroscopic Observations*

As the macroscopic properties of UHPC are closely related to its microstructure, rights after remoulding all specimens were evaluated visually. Macroscopic observations revealed that the samples initially hardened under higher pressure had significantly less air voids. If there were clearly visible pores for samples hardened without pressure, for samples initially hardened under the pressure of 50 MPa the situation was completely opposite and no pores at a macroscopic level were observed. Even for the specimens initially hardened under the pressure of 10 MPa very few macroscopic defects were noticed (Left specimen in Fig. 3).

Fig. 3. Looking from the left: the specimens prepared by applying the pressure of 10; 30 and 50 MPa.

### *Material Density*

Densities of the specimens were observed carefully in order to control pressure application process. Measured densities for samples hardened under different pressure levels are shown in Fig. 4.

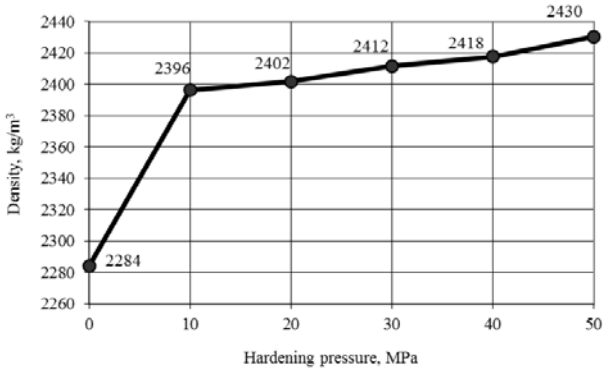


Fig. 4. Density of the 28-day-old specimens depending on hardening pressure applied.

Two different regions can be clearly distinguished: samples hardened without pressure and samples initially hardened under the pressure of 10–50 MPa. Figure 4 shows that the most significant increase in density is observed, when pressure is increased from 0 to 10 MPa indicating removal of most of the entrapped air from the specimens. In the next interval, when pressure ranges from 10 to 50 MPa, density increases almost linearly, but the average increase rate is 7.6% of that observed in the first interval. Conclusion can be drawn that for concrete with cone slump class S2, the pressure of 10 MPa is sufficient to eliminate most of entrapped air and excess water. By increasing pressure above 10 MPa, micro- and nanoscale pore volume decreases.

### *B. Compressive Strength*

Compressive strength was tested at the age of 28 days and 6 months. The results of compressive strength at 28 days are given in Figure 5. Samples without pressure application reached the compressive strength of 103.9 MPa. Samples to which 50 MPa pressure was applied reached the compressive strength of 153.6 MPa corresponding to the strength increase of 48%. Every 1MPa of pressure applied to the sample in the first 24 hours gave an average extra 1 MPa of compressive strength after 28 days of hardening. When the pressure of 10 MPa was applied, this rate was three times higher. Pressure up to 10 MPa might be practically applied in the pre-cast concrete industry, higher pressure value could be technologically difficult to achieve for the real concrete elements. The smaller the distance between concrete particles, the lower porosity, the higher density and the higher compressive strength after 28 days was reached. Compressive strength increased considerably after 6-month hardening period. Compressive strength for samples initially hardened under the pressure of 50 MPa was 174.2 MPa (14% increase compared to 28-day compressive strength).

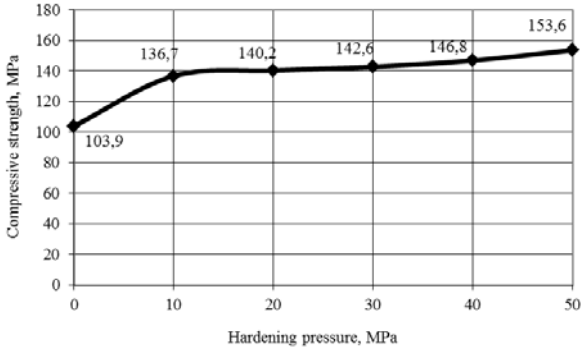


Fig. 5. Compressive strength of the 28-day-old specimens depending on hardening pressure applied.

*C. Porosity*

Main factors responsible for the porosity reduction of UHPC here are the following: low water/cement ratio, the presence of silica fume acting as pozzolan and filler, as well as pressure applied to the specimens during initial hardening in order to remove the entrapped air.

Porosity of samples was determined at the age of 28 days and 6 months. To obtain more detailed information, three different techniques were used. First, material density and specific gravity were measured and total porosity was calculated as a difference between the two. Specific gravity was determined by a pycnometer method. Second, pores in the range of 0.0064–950 μm were measured by the mercury intrusion porosimeter "Pore Master 33" from "Quantachrome Instruments". Third, pores in the range of 0.35–200 nm were measured by the gas sorption porosimeter "NOVA 1200E" from "Quantachrome Instruments". Different methods for pore structure investigation were used, for example, MIP is more suitable to measure capillary porosity and gas sorption – to measure the finest pores more accurately as suggested by J. Thomas and H. Jernnings [14]. Finally, structure of porosity was also observed by the scanning electron microscope. Results calculated from material density and specific gravity are displayed in Fig. 6. By increasing pressure from 0 to 10 MPa, porosity rapidly decreased from 7.8%–3.3%. By increasing pressure from 10 MPa to 50 MPa, porosity decreased at an average rate of only 7% of that observed in the first interval reaching 1.9% for the pressure of 50 MPa. The rapid porosity decrease in the interval

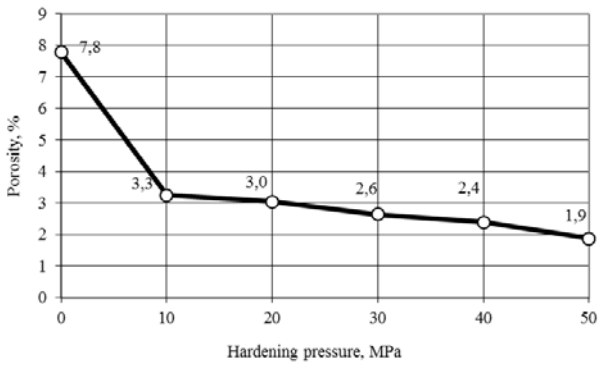


Fig. 6. The total porosity of the 28-day-old specimens depending on hardening pressure applied

0 – 10 MPa could be explained by the fact that the calculated porosity results also included macroscopic defects and relatively small pressure was necessary to eliminate macroscopic air voids. However, significantly higher pressure is required to reduce the micro- and nanoscale pore size volume.

A certain amount of air usually gets entrapped in concrete during the mixing operations [15]. Entrapped air voids usually are in the range from 0.1 to 10 mm; they are much bigger than capillary voids and are capable of adversely affecting the strength. In accordance with Mehta, pores of tested specimens can be referred as micropores and mesopores and there are a number of pores, which can be attributed as capillary pores [16]. Silva [9] made the classification of pore sizes in hydrated cement paste and determined properties affected by them: pores in the hydrated phases ("gel") of less than 10 nm can influence shrinkage and creep, medium size capillaries of 10–50 nm are responsible for strength, permeability, creep, and shrinkage at high relative humidity, large capillaries (50 nm–1 μm) affect strength and permeability, and entrained and entrapped air voids larger than 1 μm have a strong influence on the strength of specimens.

Air voids were also detected and their diameters were evaluated visually from SEM images. Only a few pores of more than 200 nm in diameter were observed by SEM for the samples to which pressure was applied (Fig. 7).

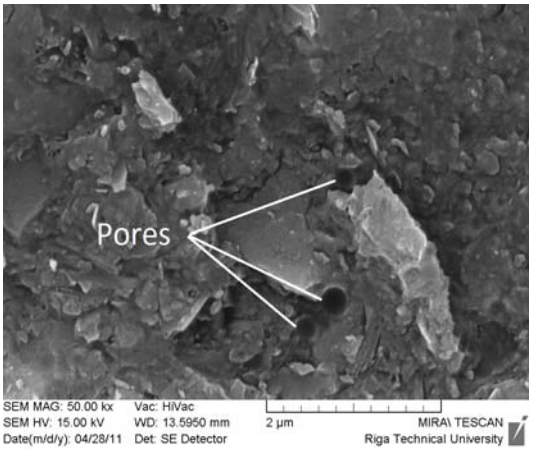


Fig. 7. SEM micrograph of concrete hardened under pressure of 50 MPa

The porosity was tested by mercury intrusion porosimetry (MIP) method, where the porosity of the specimen was measured by non-wetting liquid (mercury) intrusion in the material.

The total porosity measured by MIP for 28-day-old sample with applied pressure of 50 MPa was 1.89% that conforms well to the total porosity (1.9%) calculated from material density and spacific gravity (Fig. 6). The total open porosity (interparticle porosity) was 0.63% and total closed porosity (intraparticle porosity) was 1.26%. For 6-month-old specimens, total interparticle porosity was the same 0.63%, but total intraparticle porosity decreased to 0.97%. Total porosity of 6-month-old sample decreased to 1.6%. However, P.H. Metha [16] points out that pore size distribution is a better criterion to evaluate characteristics of a hydrated cement

paste rather than total capillary porosity. Capillary voids larger than 50 nm are more influential in determining the strength and permeability characteristics of concrete, and this conforms to the results obtained in this study: the compressive strength of specimens initially hardened under the pressure of 50 MPa increased from 153 MPa at 28 days to 174 MPa at 6 months as hydration proceeded and finer porosity was created. Obtained pore size distribution for 28-day- and 6-month-old samples with applied pressure of 50 MPa is shown in Fig. 8.

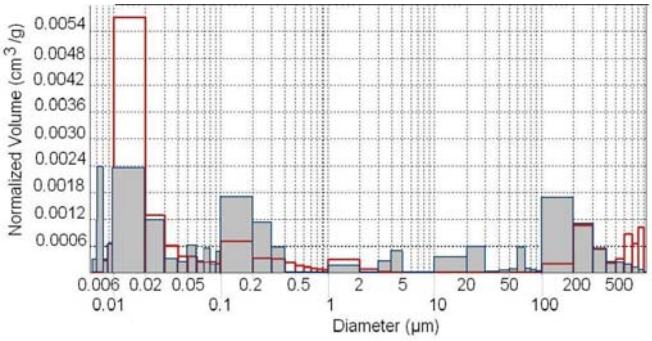


Fig. 8. Pore volume histogram of 28-day-old specimen (line) and 6-month-old specimen (grey coloured volume) initially hardened under the pressure of 50 MPa.

Pore diameters for both 28-day-old specimen and 6-month-old specimen ranged from 950 µm to 6 nm. The maximum concentration of pores for both specimens was in the range of 6–30 nm and in the range of 100-950 µm. The total pore volume decreased for a specimen cured for 6 months, and it corresponded to SEM images, where denser microstructure was observed.

Sample with applied pressure of 20 MPa at the age of 6 months demonstrated the total porosity of 2.97% (for the sample to which pressure of 50 MPa was applied it was 1.6%). Interparticle porosity was 0.67% and intraparticle porosity – 2.30%. Pore volume histogram can be seen in Fig. 9.

Mehta states that the capillary voids may range from 10–50 nm in the well-hydrated, low w/c ratio pastes [16]. In this study, pores in the range of 6 to 20 nm and 100 to 950 mµ were dominant. Ye [17] suggests that pores in concrete depending on their size and influence on performance of concrete can be classified as follows: harmless pores (<20 nm), few-harm pores (20–50 nm),

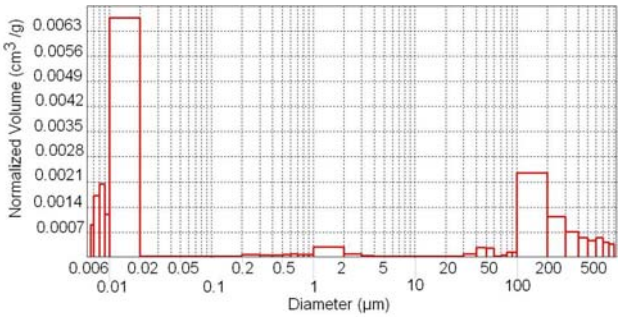


Fig. 9. Pore volume histogram of 6-month-old specimen hardened under the pressure of 20 MPa.

harmful pores (50–200 nm) and multi-harm pores (>200 nm). According to Figures 10 and 11, almost half of the porosity volume can be regarded as harmless pores as they are smaller than 20 nm.

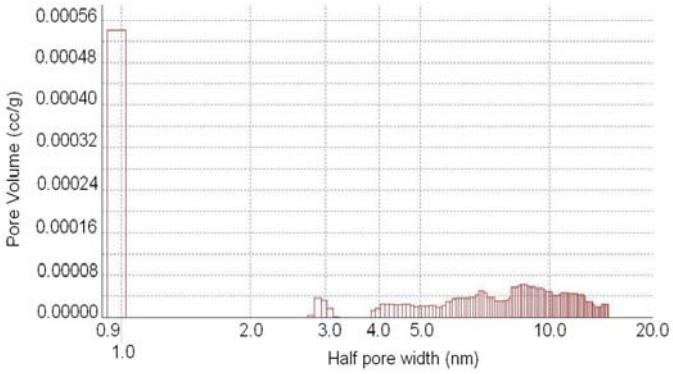


Fig. 10. Pore volume histogram of 28-day-old specimen hardened under the pressure of 50 MPa.

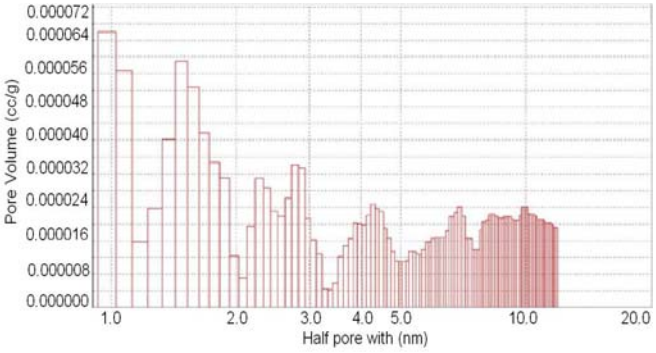


Fig. 11. Pore volume histogram of 6-month-old specimen initially hardened under the pressure of 50 MPa.

However, Mehta [16] notes that voids smaller than 50 nm, referred to as micropores, play an important role in drying shrinkage and creep. In order to get a better understanding of the hydration process of cement paste initially hardened under pressure, the micropore size distribution was determined by gas sorption porosimeter. According to the obtained data, cumulative volume of micropores for 28-day-old specimen initially hardened under the pressure of 50 MPa was $4.38 \times 10^{-3}$ $cm^3/g$. According to the pore volume histogram, two types of pores can be distinguished – very small micropores with radius from 0.9 to 1 nm and micropores with radius in the range from 4 to 18 nm (Fig. 10).

Data for 6-month-old specimen initially hardened under the pressure of 50 MPa showed that cumulative volume of micropores was reduced twice ($2.38 \times 10^{-3} cm^3/g$) compared to the 28-day-old specimen ($4.37 \times 10^{-3}$ $cm^3/g$). The number of pores of 1 nm considerably decreased as their volume decreased almost 8 times from $5.6 \times 10^{-4}$ $cm^3/g$ to $0.7 \times 10^{-4}$ $cm^3/g$. Possible explanation for this could be the formation of a more dense crystalline structure during a prolonged curing period.

*Microscopic (SEM) Observations of Concrete Initially Hardened under the Pressure of 50 MPa*

The sample fracture surfaces after compressive strength tests of 28 day- and 6-month-old concrete specimens (pressure of 50 MPa) were observed by the scanning electron microscope TESCAN Mira\LMU. Samples were taken from the middle of crushed specimens. The microstructure of 6-month-old specimen initially hardened under the pressure of 50 MPa prevalently looked denser and more homogenous compared to that of 28-day-old specimen (Fig. 12 and 13).

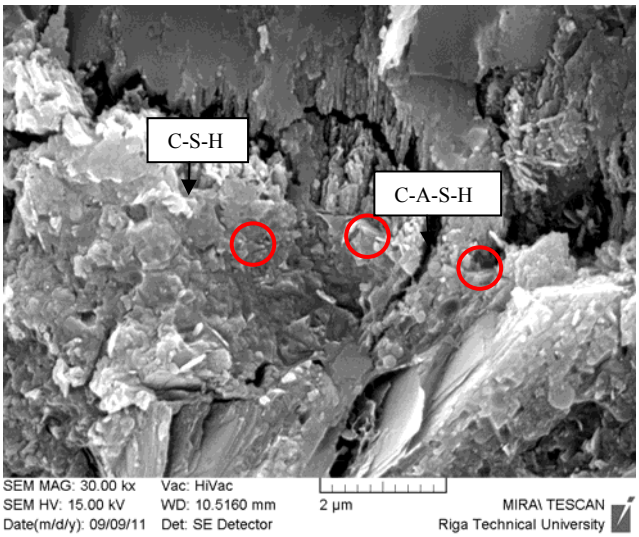


Fig. 12. SEM micrograph of 28-day-old specimens initially hardened under the pressure of 50 MPa: monosulfate hydrate, $C_4ASH_{18}$ (C-A-S-H), calcium silicate hydrates (C-S-H). Particles of silica fume are marked in the micrograph.

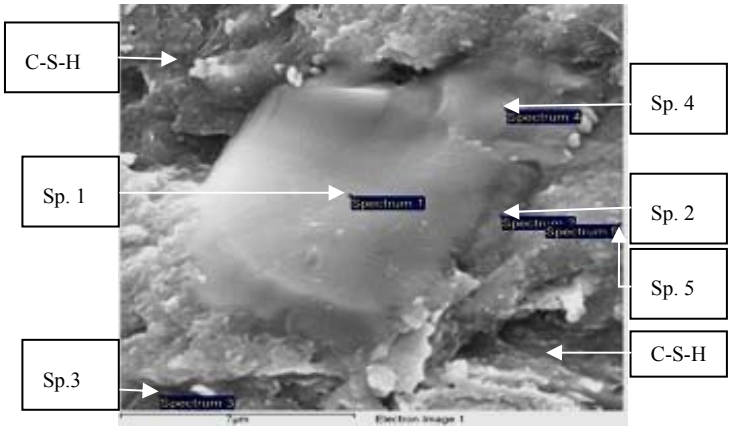


Fig. 13. SEM micrographs of 6-month-old specimens initially hardened under the pressure of 50 MPa: calcium silicate hydrates (C-S-H).

It seems that microstructure of 28-day-old concrete is under development and is not completely settled. The morphology of C-S-H of 28-day-old specimen becomes denser through the formation or transformation of crystals in the solid state during time period of 6 months. Amplification of compressive strength (14% increase compared to 28-day compressive strength approved it) and investigation of pore structure (cumulative volume of micropores reduced almost twice) of 6 month-old samples initially hardened under the pressure of 50 MPa proved the hypothesis about structural changes in the solid state.

Investigations done by scanning electron microscope (SEM) probably showed a strong retardation of the hydration process caused by an extremely low water-cement ratio and high pressure application in the time period of initial hardening of concrete. The hydration process of early stage was not investigated in this research.

The morphology of C-S-H seems different compared to traditional concrete due to low water-cement ratio of UHPC (w/c = 0.25). It has already been proven that the chemical composition and morphology of the calcium silicate hydrates in hydraulic Portland cement pastes vary with the water-cement ratio, temperature and age of hydration. The pressure which was applied during the initial hardening process can also strongly influence the morphology of C-S-H. In the micrographs, two apparently different types or morphologies of C-S-H can be seen. One of them is more porous and appears in the first stage of hardening process (Fig. 12), while the other looks denser and more amorphous (Fig. 13). According to literature [14], the less dense morphology of S-C-H forms rapidly during the early hydration period around concrete setting, while the denser morphology appears more slowly over days and weeks. Based on these characteristics, the two types have been given a variety of distinguishing labels, including "early" and "late", "outer" and "inner". Thomas and Jernnings prefer the terms "low-density" and "high-density" C-S-H, because the other terms are only approximately correct (i.e., some low-density C-S-H can form later and some high-density C-S-H is found outside the original particle boundaries) [14]. Microstructure of “low-density" and "high-density" C-S-H of UHPC could be characterized by a size of gel pores. The gel pores normally are smaller than 10 nm. Volume of pores in the microstructure of specimen hardened for a longer time period decreased due to prolonger hydration of cement paste and C-S-H transformation from “low-density" to "high-density". The number of gel pores smaller than 1 nm considerably decreased as their volume decreased almost 8 times if comparing 28-day- and 6-month-old specimens initially hardened under the pressure of 50 MPa. Possible explanation of this could be the formation of a more dense crystalline structure during a prolonged curing period. Size and volume of gel pores should also be affected by pressure in the time period of initial hardening. SEM images of the present section confirm this observation.

According to the EDX investigations (Table 3), dense crystals typical of 6-month-old specimens initially hardened under the pressure of 50 MPa were found as modifications of C-S-H (Fig. 13). Spectrum 3 contains small amount of S, and monosulfate hydrate could possibly be found there. Such elements as Fe, Mg, Al, Ti, and K, which come from Portland cement (Table 1) and go into composition of C-S-H, were detected. The microphotographs describe a common structure of UHP concrete hardened for 6 months (Fig. 13).

TABLE III
EDX RESULTS ILLUSTRATED BY FIGURE 13, ATOMIC WEIGHT %

| Elements | Spectrum | | | | |
|---|---|---|---|---|---|
| | 1 | 2 | 3 | 4 | 5 |
| O | 46.03 | 56.76 | 58.51 | 54.02 | 63.63 |
| Mg | 0.33 | 0.87 | 0.39 | 0.85 | 0.27 |
| Al | 0.41 | 3.93 | 1.54 | 11.3 | 1.73 |
| Si | 9.58 | 10.48 | 16.42 | 2.92 | 21 |
| S | | | 0.87 | | |
| K | | 0.27 | 0.49 | 1.04 | 0.58 |
| Ca | 43.65 | 23.67 | 21.12 | 25.76 | 12.79 |
| Ti | | 0.31 | | | |
| Fe | | 3.71 | 0.67 | 4.12 | |
| Total | 100.00 | 100.00 | 100.00 | 100.00 | 100.00 |

### *D. Mineralogical Composition*

Mineralogical composition was obtained by XRD analysis method for two specimens: the specimens initially hardened under the pressure of 50 MPa were tested at the age of 28 days and 6 months. The fact that the term C-S-H is hyphenated signifies that C-S-H is not a well-defined compound; the C/S ratio varies between 1.5 and 2.0 and structural water content varies even more. The morphology of C-S-H also varies from poorly crystalline fibres to a reticular network. Due to their colloidal dimensions and tendency to cluster, C-S-H could only be resolved with the advanced electron microscopy. In older literature, the material is often referred to as C-S-H gel with an amorphous structure [16]. Due to pressure application in the time period of initial setting of specimens and low water-cement ratio, C-S-H formed in the amorphous phase, which was not detected by XRD analysis.

No typical phase of calcium hydroxide (CH) was found due to high silica fume content, which in reaction with CH formed C-S-H phase. Pozzolanic reactions between silica fume and free CH form C-S-H and reduce the amount of CH in hydrated cement paste.

Amount of larnite slightly decreased for 6-month-old specimen due to the prolonged hydration of cement grains.

Main minerals, which were detected by XRD, were minerals from fillers and aggregates used in the production of concrete. Dolomite, calcite, microline, quartz, plagioclase are typical minerals of Latvian sand. Sand fraction 0.3/2.5 mm contains dolomite grain particles. Microline and plagioclase are formed from degradation of feldspar. Calcium carbonate and quartz were present in sand. Larnite is dicalcium silicate, which is partially hydrated cement mineral; otherwise XRD analysis would not identify such mineral.

## IV. Conclusions

Pressure of 10, 20, 30, 40 and 50 MPa was applied to the concrete specimens during initial hardening (24 hours) in order to improve physical and mechanical properties of the materials. Compressive strength, density and microstructure were investigated. Several conclusions can be drawn from this study. By applying pressure in the initial phase of concrete hardening, it is possible to achieve UHPC compressive strength border (150 MPa) for the concrete mixes with normal cement and without fibres, which normally at the age of 28 days achieve only 100 MPa. The greatest gain in concrete performance characteristics was observed in the first pressure step of 10 MPa (strength increased by 31.5%). By increasing pressure further to 50 MPa, slower enhancement of the concrete properties was noticed.

Due to application of the pressure of 50 MPa, density of samples increased from 2284 kg/m$^3$ to 2430 kg/m$^3$, porosity decreased from 7.8% to 1.9%. Significant gain of compressive strength of 48% (103.9 to 153.6 MPa) was observed. After 6 months, compressive strength increased by 14% compared to that of 28 days reaching 174.2 MPa.

Pore structure analysis indicated that concrete samples hardened under higher pressure had significantly lower pore volume and overall pore size decreased. Porosity was decreased from 7.8% to 1.9% by application of the pressure of 50 MPa. Total interparticle porosity did not change after 6-month hardening and was the same as at 28 days – 0.63%; however, the pore size distribution changed considerably (pore sizes decreased). Intraparticle porosity decreased from 1.26% at 28 days to 0.97% at 6 months, resulting in a denser matrix and the increased compressive strength.

SEM images revealed a much denser microstructure of 6-month-old sample than that of 28-day-old sample.

At the age of 28 days, partially reacted silica fume particles were observed in the samples. After 6 months, a smaller number of partially reacted silica fume particles were present in the microstructure of UHPC according to microphotographs.

Practically, pressure application during the concrete setting could be used in precast element fabrication. Probably it would be possible to apply pressures up to 10 MPa.

Summarizing the results it can be concluded that pressure is an effective instrument to decrease concrete porosity and achieve high mechanical strength and high performance characteristics of concrete.

## Acknowledgements

The financial support of the ERAF project No.2010/0286/2DP/2.1.1.1.0/10/APIA/VIAA/033 "High Efficiency Nanoconcrete" is highly acknowledged.

## References

[1] P.C. Aitcin, *High Performance Concrete*. E and FN: Spon, London, 1998.

[2] A. Jain, "High Performance Concrete Research and Practice", Proc. Construction Management and Materials, I.I.T, 2003, Kharagpur, Jan 9-11, p. 450–560.

[3] K.H. Khayatand, P.C. Aitcin, "Silica fume in concrete: an overview", Fourth CANMET/ACI International Conference on Fly ash, Silica fume, slag and natural pozzolans in concrete, SP-132, V.2.1992. 835. Guide for use of silica fume, 1996, 234R-96 ACI Publications.

[4] R. Khurana, "Admixtures for ready mixed high strength and durable concrete ERMCO", 12th European Congress, 1998.

[5] P. Richard, M. H. Cheyrezy, *Reactive powder concretes with high ductility and 200-800 N/mm2 compressive strength.Metha, P.K(ed.)*. Concrete Technology: Past, Present and Future, SP144-24, 1995, pp. 507–517.

[6] P. Richard, M. Cheyrezy, "Composition of reactive powder concretes", Cement and Concrete Research, vol. 25, no. 7. pp. 1501–1511, 1995.

[7] E. Fehling, K. Bunje, M., Schmidt, W. Schreiber, "Ultra High Performance Composite Bridge across the River Fulda in Kassel–

Conceptual Design", Design Calculations and Invitation to Tender. Proceedings of the International Symposium on Ultra High Performance Concrete, 2004, Kassel, p. 69–75.
[8] D.R. Dinger J.E. Funk, "Particle Packing II-Review of Packing of Polydisperse Particle Systems", Interceram. 41/2, 1992, p. 95–97.
[9] D.A. Silva, V.M. John, J.L.D. Ribeiro, H.R. Roman, "Pore size distribution of hydrated cement pastes modified with polymers", Cement and Concrete Research, vol.31, issue 8, 2001, p.1177–1184.
[10] Z. Hajar, D. Lecointre, A. Simon, J. Petitjean, "Design and Construction of the world first Ultra-High Performance Concrete road Bridges", Proceedings of the International Symposium on Ultra High Performance Concrete, 2004, Kassel, p. 39–48.
[11] P. Acker, M. Behloul, "Ductal® Technology: a Large Spectrum of Properties, a Wide Range of Applications" Proceedings of the International Symposium on Ultra High Performance Concrete, Kassel, 2004, p. 9–23.
[12] M.E. Freyssinet, *Cement and Concrete Manufacture*, vol. 9, 1936, pp. 71.
[13] A. M. Neville, *Properties of concrete, 4th ed*. England: Longman group limited, 1995.
[14] H. Jennings, J. J. Thomas, *Materials of cement science primer*. Northwestern University: Evanston, 2009.
[15] R.C., Mielenz, V.E., Wolkodoff, J.E. Backstrom, H.I. Flack, "Origin, Evolution, and Effects of the Air Void System in Concrete". Part 1 – Entrained Air in Unhardened Concrete, *Journal*, American Concrete Institute, July 1958; *Proceedings*, vol. 55; "Part 2—Influence of Type and Amount of Air-Entraining Agent," *Journal*, American Concrete Institute, August 1958; *Proceedings*, vol. 55; "Part 3—Influence of Water-Cement Ratio and Compaction," *Journal*, American Concrete Institute, October 1958; *Proceedings*, vol. 55.
[16] P.K. Mehta, P.J.M. Monteiro, "Hight performance concrete; from material to structure, The McGraw-Hill companies", Inc. 2006.
[17] Q. Ye, *New Build. Materials*. pp. 4–6 (1), 2001.

**Janis Justs**, Doctoral student at Riga Technical University, the Faculty of Civil Engineering, Research Assistant, Riga Technical University, Institute of Materials and Structures, Professor's Group of Building Materials and Wares.
Address: 1 Kalķu Str., Riga, LV–1658, Latvia. E-mail: janis.justs@rtu.lv

**Diana Bajare**, Dr.sc.ing., Assoc. prof., Riga Technical University, Institute of Materials and Structures, Professor's Group of Building Materials and Wares.
Address: 1 Kalķu Str., Riga, LV–1658, Latvia. E-mail: diana.bajare@rtu.lv

**Aleksandrs Korjakins**, Dr.sc.ing., Prof., Riga Technical University, Institute of Materials and Structures, Professor's Group of Building Materials and Wares.
Address: 1 Kalķu Str., Riga LV–1658, Latvia. E-mail: aleks@latnet.lv

**Janis Locs**, Dr.sc.ing., Riga Technical University, Riga Biomaterials Innovation and Development Centre.
Address: Pulka Str. 3/3, Riga, LV–1007, Latvia. E-mail: janis.locs@rtu.lv

**Gundars Mezinskis**, Dr.habil.sc.ing., Prof., Riga Technical University, Institute of Silicate Materials.
Address: 1 Kalķu Str., Riga, LV–1658, Latvia. E-mail: gundarsm@ktf.rtu.lv

**Girts Bumanis**, BSc.Ing., Research Assistant, Riga Technical University, Institute of Materials and Structures, Professor's Group of Building Materials and Wares.
Address: 1 Kalķu Str., Riga, LV–1658, Latvia. E-mail: girts.bumanis@rtu.lv